Discovery Prospects for a Leptophilic Gauge Boson Z_{ℓ} at CEPC and ILC

S.O. Kara

Niğde Ömer Halisdemir University, Bor Vocational School, 51240, Niğde, Türkiye

Abstract: We investigate the discovery prospects of a leptophilic gauge boson Z_ℓ at future e^+e^- colliders, focusing on a comparative study of the Circular Electron–Positron Collider (CEPC) and the International Linear Collider (ILC). Such a state naturally arises from an additional $U(1)'_\ell$ gauge symmetry, under which quarks remain neutral while all leptons carry a universal charge, motivated by neutrino oscillations and scenarios of physics beyond the Standard Model (SM). As a clean benchmark, we study the process $e^+e^- \to \mu^+\mu^-$, including realistic effects of initial-state radiation (ISR) and beamstrahlung (BS). Our results indicate that CEPC, with its very high luminosity at $\sqrt{s} = 240$ GeV, can probe couplings down to $g_\ell \approx 10^{-3}$ for Z_ℓ masses up to about 220 GeV, while the ILC extends the sensitivity to heavier states in the multi-hundred GeV range through its higher \sqrt{s} stages. These findings demonstrate the strong complementarity of circular and linear colliders in exploring purely leptophilic interactions.

Keywords: Leptophilic gauge boson, Z_{ℓ} , CEPC, ILC, electron–positron collider, beyond Standard Model

DOI: CSTR:

I. INTRODUCTION

The Standard Model (SM) of particle physics has been remarkably successful in describing the fundamental constituents of matter and their interactions [1]. Nevertheless, the observation of neutrino oscillations [2, 3] and the violation of individual lepton flavor numbers clearly point towards new physics beyond the SM. Among the simplest and most intriguing possibilities is the existence of an additional abelian gauge symmetry under which quarks remain neutral while all leptons carry a universal charge. Such a symmetry is particularly well motivated by the fact that neutrino oscillations already require new dynamics in the lepton sector, suggesting that leptons may play a privileged role in extensions of the SM. In addition, the $U(1)'_{\ell}$ construction is anomaly-free when all lepton families are assigned identical charges, providing a theoretically consistent and minimal extension of the gauge structure. The associated gauge boson, conventionally denoted as the leptophilic photon Z_{ℓ} , couples exclusively to leptons and thus realizes a genuinely leptophilic interaction [4-10].

Electron-positron colliders provide an ideal environment to probe this kind of new physics due to their clean experimental conditions and well-defined initial states. In particular, the upcoming Circular Electron-Positron Collider (CEPC) [11] and the International Linear Collider (ILC) [12] represent two complementary approaches for the next generation of lepton colliders. While the CEPC aims at extremely high luminosity around the Higgs fact-

ory energy, the ILC offers the flexibility of operating at both $\sqrt{s} = 250$ GeV and 500 GeV, thereby extending the reach into the TeV regime. This complementarity renders them powerful and mutually reinforcing facilities to explore new leptophilic interactions.

Beyond the general motivation, it is worth stressing that CEPC and ILC offer complementary advantages that have not yet been systematically compared in the leptophilic context. Earlier works have focused either on generic Z' scenarios including quark couplings or on simplified parton-level estimates for purely leptophilic interactions [7, 8], without incorporating realistic collider and detector effects. By contrast, the present study includes both initial-state radiation (ISR) and beamstrahlung (BS) as well as acceptance cuts, thereby providing sensitivity projections that are directly applicable to the experimental programs of CEPC and ILC.

Moreover, the comparison is timely in view of the global strategy for future colliders. CEPC has been highlighted as a central project in China, designed to operate as a Higgs factory with unprecedented luminosity, while the ILC has received strong international attention as a linear machine with higher center-of-mass energy options. Establishing the relative strengths of these colliders in probing leptophilic gauge interactions is therefore not only of theoretical interest but also of practical importance for optimizing the physics reach of upcoming facilities. This complementarity is particularly relevant since hadron colliders have very limited sensitivity to leptophilic states, making lepton machines unique labor-

Received 17 September 2025; Accepted 11 November 2025

^{©2026} Chinese Physical Society and the Institute of High Energy Physics of the Chinese Academy of Sciences and the Institute of Modern Physics of the Chinese Academy of Sciences and IOP Publishing Ltd. All rights, including for text and data mining, AI training, and similar technologies, are reserved.

atories for such searches.

Taken together, these considerations underline both the novelty and the significance of the present analysis. Our results provide the first direct, side-by-side comparison of CEPC and ILC capabilities for discovering a leptophilic photon, and thus contribute to the broader discussion of physics opportunities at next-generation lepton colliders.

In this work, we present a comparative phenomenological study of the discovery potential for the leptophilic photon Z_{ℓ} at CEPC and ILC, focusing on the clean channel $e^+e^- \to \mu^+\mu^-$. We evaluate the expected sensitivities by incorporating realistic effects of ISR, BS, and detector acceptance. This channel provides a distinctive signature with minimal SM background and therefore constitutes an optimal probe of purely leptophilic interactions. In this way, our analysis extends previous parton-level estimates [7, 8] and offers a more reliable assessment of the capabilities of future e^+e^- colliders.

II. THEORETICAL FRAMEWORK

A minimal and economical way to extend the Standard Model (SM) is to introduce an additional abelian gauge symmetry $U(1)'_{\ell}$ under which all leptons carry a universal charge, while quarks remain neutral. This idea dates back to early studies of generalized gauge structures [13–15] and has been revisited in various contexts of leptophilic or leptonic interactions [8, 9, 16]. The new gauge boson, denoted Z_{ℓ} , couples exclusively to leptons and therefore realizes a genuinely leptophilic interaction.

The covariant derivative is modified to include the new gauge interaction,

$$D_{\mu} = \partial_{\mu} + ig_{\ell}' q_{\ell} Z_{\mu}', \tag{1}$$

where g'_{ℓ} is the gauge coupling constant, q_{ℓ} the universal lepton charge, and Z'_{μ} the new gauge field. The relevant terms of the Lagrangian read

$$\mathcal{L} \supset -\frac{1}{4} F'_{\mu\nu} F'^{\mu\nu} + \bar{\ell} i \gamma^{\mu} D_{\mu} \ell + (D_{\mu} \Phi)^{\dagger} (D^{\mu} \Phi) - V(\Phi), \qquad (2)$$

where Φ is a scalar field charged under $U(1)'_{\ell}$ whose vacuum expectation value (vev) spontaneously breaks the new symmetry, thereby generating a mass for the leptophilic boson Z_{ℓ} .

The interaction between Z_{ℓ} and the leptonic current can be expressed as

$$\mathcal{L}_{\text{int}} = g_{\ell} Z_{\ell,\mu} J_{\text{lep}}^{\mu}, \qquad J_{\text{lep}}^{\mu} = \sum_{\ell = e, \mu, \tau} \bar{\ell} \gamma^{\mu} \ell, \tag{3}$$

which highlights the universal coupling of Z_{ℓ} to all

charged leptons. A crucial theoretical requirement is the absence of gauge anomalies, which would otherwise spoil the consistency of the theory at the quantum level [17–20]. In the present setup, anomalies cancel if all three lepton families are assigned the same $U(1)'_{\ell}$ charge. With this choice, the $[SU(2)_W]^2U(1)'_{\ell}$, $[U(1)_Y]^2U(1)'_{\ell}$, and $[U(1)'_{\ell}]^3$ anomalies vanish.

Mixing effects can in principle arise in two ways. First, kinetic mixing with the hypercharge gauge boson B_{μ} may occur through

$$\mathcal{L}_{\text{mix}} = -\frac{\epsilon}{2} F_{\mu\nu}^{Y} F^{\prime\mu\nu},\tag{4}$$

where ϵ parametrizes the mixing strength. Such terms are typically induced at loop level [14], but precision electroweak data require $\epsilon \lesssim 10^{-2}$ [7]. Recent works [21] have studied electroweak precision constraints in nearly-degenerate Z'-Z systems, showing that even small kinetic and mass mixing generate observable shifts in the oblique parameters S, T, U, consistent with existing data. Second, after electroweak symmetry breaking, the SM Z boson and the new Z_{ℓ} can mix via the scalar sector. The mass-squared matrix in the (Z, Z_{ℓ}) basis is

$$M^2 = \begin{pmatrix} M_Z^2 & \delta M^2 \\ \delta M^2 & M_{Z_I}^2 \end{pmatrix},\tag{5}$$

with δM^2 induced by the vev of Φ . Further studies [22] computed corrections to electroweak observables from such mixings in the context of anomalies like the W-boson mass shift, finding constraints that closely match the $\theta \lesssim 10^{-3}$ limit. In the parameter space of interest here, both kinetic and mass mixing are negligible, so Z_{ℓ} couples purely to leptons at tree level. Model-independent analyses [23] further support the treatment of mixing effects as subdominant for the benchmark values considered here

Constraints from precision electroweak measurements imply a lower bound on the ratio between the new boson mass and its coupling,

$$\frac{M_{Z_{\ell}}}{g_{\ell}} \gtrsim 7 \text{ TeV}.$$
 (6)

Representative exclusion limits on g_{ℓ} for benchmark masses are summarized in Table 1. Electroweak precision data require $g_{\ell} \lesssim 1.4 \times 10^{-2}$ at $M_{Z_{\ell}} \sim 100$ GeV, with the bound gradually relaxing to $O(10^{-1})$ in the multi-TeV regime.

Altogether, the framework is anomaly-free, predictive, and renormalizable. The Z_{ℓ} couples universally to leptons, has negligible couplings to quarks, and only tiny mixing with SM gauge bosons. These features make fu-

Table 1. 95% C.L. exclusion limits on the leptophilic coupling g_{ℓ} from electroweak precision fits.

| $M_{Z_{\ell}}$ [GeV] | Limit on g_ℓ | | |
|----------------------|------------------------|--|--|
| 100 | $< 1.4 \times 10^{-2}$ | | |
| 240 | $< 3.4 \times 10^{-2}$ | | |
| 250 | $< 3.6 \times 10^{-2}$ | | |
| 500 | $< 7.1 \times 10^{-2}$ | | |
| 1000 | $< 1.4 \times 10^{-1}$ | | |
| 3000 | $< 4.3 \times 10^{-1}$ | | |

ture high-luminosity lepton colliders the ideal environment to search for Z_{ℓ} , as hadronic machines are comparatively much less sensitive.

III. COLLIDER SETUP

To assess the sensitivity to leptophilic interactions at future e^+e^- machines, we base our analysis on the baseline beam parameters summarized in Table 2. For CEPC we adopt the design values reported in the Conceptual Design Report (2018) [11], and for the ILC we follow the Technical Design Report (2013) [12]; these choices are consistent with Ref. [24]. Throughout, σ_x and $\sigma_{\rm v}$ denote the horizontal and vertical root-mean-square (rms) beam sizes at the interaction point (IP), σ_z the longitudinal bunch length (also an rms size, in μ m), N_b the particles per bunch (in units of 10^{10}), and L the integrated luminosity accumulated over the data-taking period. The CEPC is envisaged as a circular Higgs factory operating at $\sqrt{s} = 240 \,\text{GeV}$ with a target integrated luminosity of about 6 ab⁻¹, providing a clean environment with very high statistics for precision Higgs and electroweak studies. In contrast, the ILC is a linear collider foreseen to begin at $\sqrt{s} = 250 \text{ GeV} (1.35 \text{ ab}^{-1})$ with an upgrade path to $\sqrt{s} = 500 \,\text{GeV} \, (1.8 \,\text{ab}^{-1}) \, [12]$, thereby extending the direct kinematic reach for heavier states. Although other proposed lepton colliders such as FCC-ee [25] and CLIC [26] offer additional benchmark scenarios, they lie beyond the scope of the present CPC-focused comparison; hence, in what follows we restrict our quantitative analysis to CEPC and ILC.

In order to obtain realistic sensitivity estimates, we in-

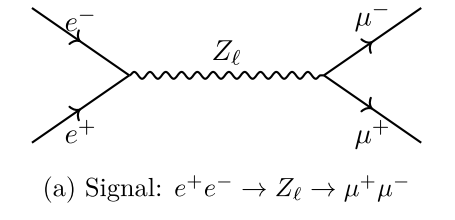


Table 2. Baseline beam parameters adopted for CEPC and ILC. Integrated luminosities are given in ab^{-1} .

| Collider | \sqrt{s} (GeV) | $L(ab^{-1})$ | σ_x (nm) | σ_y (nm) | σ_z (μ m) | $N_b \ (\times 10^{10})$ |
|----------|------------------|--------------|-----------------|-----------------|-----------------------|--------------------------|
| CEPC | 240 | 6.0 | 16.0 | 0.12 | 4.4 | 3.7 |
| ILC-250 | 250 | 1.35 | 515.0 | 7.7 | 300.0 | 2.0 |
| ILC-500 | 500 | 1.80 | 474.0 | 5.9 | 300.0 | 2.0 |

clude the effects of initial-state radiation (ISR) and beam-strahlung (BS), which modify the effective luminosity spectrum. ISR is implemented following the structure-function approach of Skrzypek and Jadach [27, 28], while BS is modeled using the official collider beam spectra provided in the design reports [29]. These effects reduce the effective collision energy and broaden the invariant-mass distributions, thereby affecting both total and differential cross sections. Throughout our study, we simulate the signal process $e^+e^- \rightarrow \mu^+\mu^-$ via $\gamma/Z/Z_\ell$ exchange and the corresponding Standard Model background using the CalcHEP framework [30–32]. Detector effects are approximated by applying acceptance cuts of $|\cos\theta_\mu| < 0.95$ and assuming high muon identification efficiency consistent with design studies.

IV. SIGNAL AND BACKGROUND ANALYSIS

The signal process considered is $e^+e^- \rightarrow \mu^+\mu^-$, mediated by Z_ℓ . This channel is particularly advantageous because the muon final state can be reconstructed with high efficiency and excellent momentum resolution, making it the cleanest probe of leptophilic interactions.

The dominant irreducible background arises from the Standard Model Drell–Yan production via photon and Z exchange, $e^+e^- \to \gamma^*/Z \to \mu^+\mu^-$. This background is theoretically well understood and experimentally clean, allowing deviations from the SM prediction to be directly attributed to the presence of a Z_ℓ contribution [33]. Reducible backgrounds from processes such as $e^+e^- \to \tau^+\tau^-$ or multihadronic final states are negligible once standard selection criteria are applied. For this reason the di-muon channel provides a uniquely sensitive and robust avenue to search for a leptophilic photon at future lepton colliders. The signal and background processes are illustrated in Fig. 1.

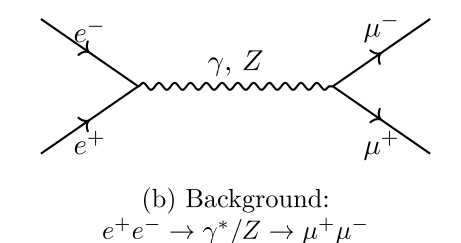


Fig. 1. Representative Feynman diagrams for the signal process $e^+e^- \to Z_\ell \to \mu^+\mu^-$ (left) and the dominant Standard Model background $e^+e^- \to \gamma^*/Z \to \mu^+\mu^-$ (right).

In our analysis, ISR and beamstrahlung effects are fully included, as discussed in the previous section. Detector-level effects are approximated by applying acceptance cuts of $|\cos\theta_{\mu}| < 0.95$ and $p_{\mu}^{T} > 10$ GeV, consistent with the design reports of CEPC and ILC. After cuts, the SM background is reduced while the Z_{ℓ} signal retains a significant fraction of events, enhancing sensitivity in the high-mass tails of distributions.

The statistical significance is evaluated using a binned likelihood method based on the invariant-mass spectrum. For each benchmark mass hypothesis, we derive exclusion limits on the coupling g_{ℓ} at 95% C.L. [34, 35] the predicted signal-plus-background spectrum with the background-only expectation. These results are presented in the following section.

The energy dependence of the total cross section is displayed in Fig. 2. At CEPC, operating at $\sqrt{s} = 240$

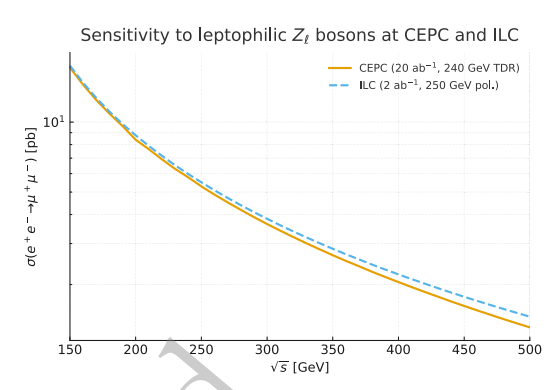


Fig. 2. (color online) Total cross section $\sigma(e^+e^- \to \mu^+\mu^-)$ as a function of the center-of-mass energy \sqrt{s} for CEPC and ILC benchmark configurations. The CEPC baseline at $\sqrt{s} = 240 \, \text{GeV}$ with $20 \, \text{ab}^{-1}$ integrated luminosity provides excellent sensitivity to light leptophilic gauge bosons, while the higher-energy ILC stages (250 and 500 GeV) extend the accessible mass range to heavier Z_ℓ states.

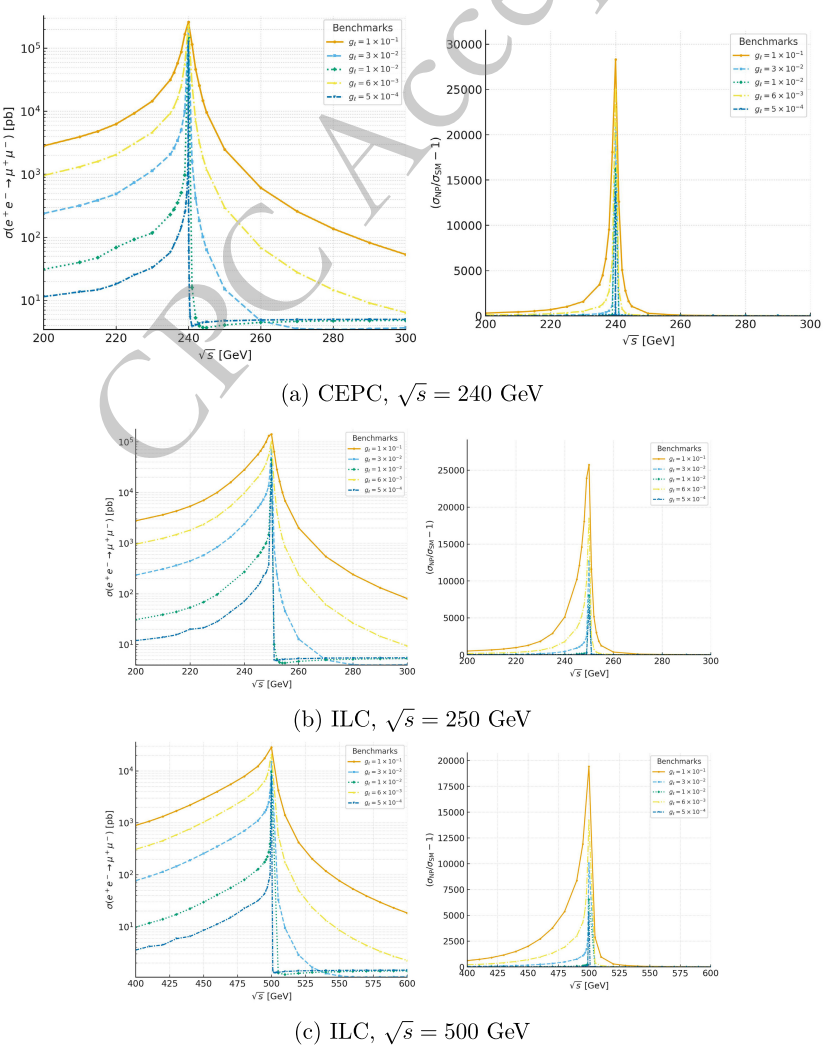


Fig. 3. (color online) Total cross section $\sigma(e^+e^- \to \mu^+\mu^-)$ and its relative deviation $(\sigma_{\rm NP}/\sigma_{\rm SM}-1)$ as functions of M_{Z_ℓ} for representative couplings g_ℓ . (a) CEPC at $\sqrt{s}=240~{\rm GeV}$ with $20~{\rm ab}^{-1}$ integrated luminosity (TDR baseline). (b) ILC at $\sqrt{s}=250~{\rm GeV}$ with $2~{\rm ab}^{-1}$ polarized beams. (c) ILC at $\sqrt{s}=500~{\rm GeV}$, where higher energies extend the sensitivity to heavier Z_ℓ states. Right-hand panels show the fractional deviation from the SM prediction, highlighting the discovery potential even for small couplings.

GeV, the high luminosity allows excellent sensitivity to deviations from the Standard Model prediction, while the ILC at $\sqrt{s} = 250$ and 500 GeV extends the accessible range in energy and probes heavier Z_{ℓ} states. The comparison illustrates the complementarity of circular and linear machines in exploring leptophilic interactions.

In Fig. 3, we show the total cross section as well as the relative deviation $(\sigma_{\rm NP}/\sigma_{\rm SM}-1)$ as functions of the new boson mass M_{Z_ℓ} for representative values of the coupling g_ℓ . The CEPC panel demonstrates that even small couplings can induce visible deviations thanks to its very high luminosity, although the accessible mass range is limited by the lower center-of-mass energy. The ILC panels illustrate how higher energies broaden the discovery potential, with the 500 GeV setup being particularly effective in probing multi-hundred-GeV Z_ℓ states. Overall, these complementary results emphasize the excellent sensitivity of future e^+e^- colliders to leptophilic gauge in-

teractions.

The dependence of the total cross section on the center-of-mass energy is illustrated in Fig. 4. The CEPC projection (Fig. 4a) shows excellent sensitivity near $\sqrt{s} = 240$ GeV due to its very high luminosity, while the ILC panels (Figs. 4b and 4c) extend the reach to higher energies. In particular, the 500 GeV configuration enhances the prospects for discovering a heavy Z_{ℓ} by probing deviations from the Standard Model spectrum well into the TeV scale.

The dependence of the total cross section on the leptophilic coupling g_{ℓ} is displayed in Fig. 5. For each collider setup, three configurations are compared: the idealized case without ISR/BS, the ISR—only case, and the full ISR+BS simulation. At the CEPC ($\sqrt{s} = 240 \text{ GeV}$), beamstrahlung has only a mild effect, while ISR dominates the suppression of the effective cross section. For the ILC, both the 250 and 500 GeV op-

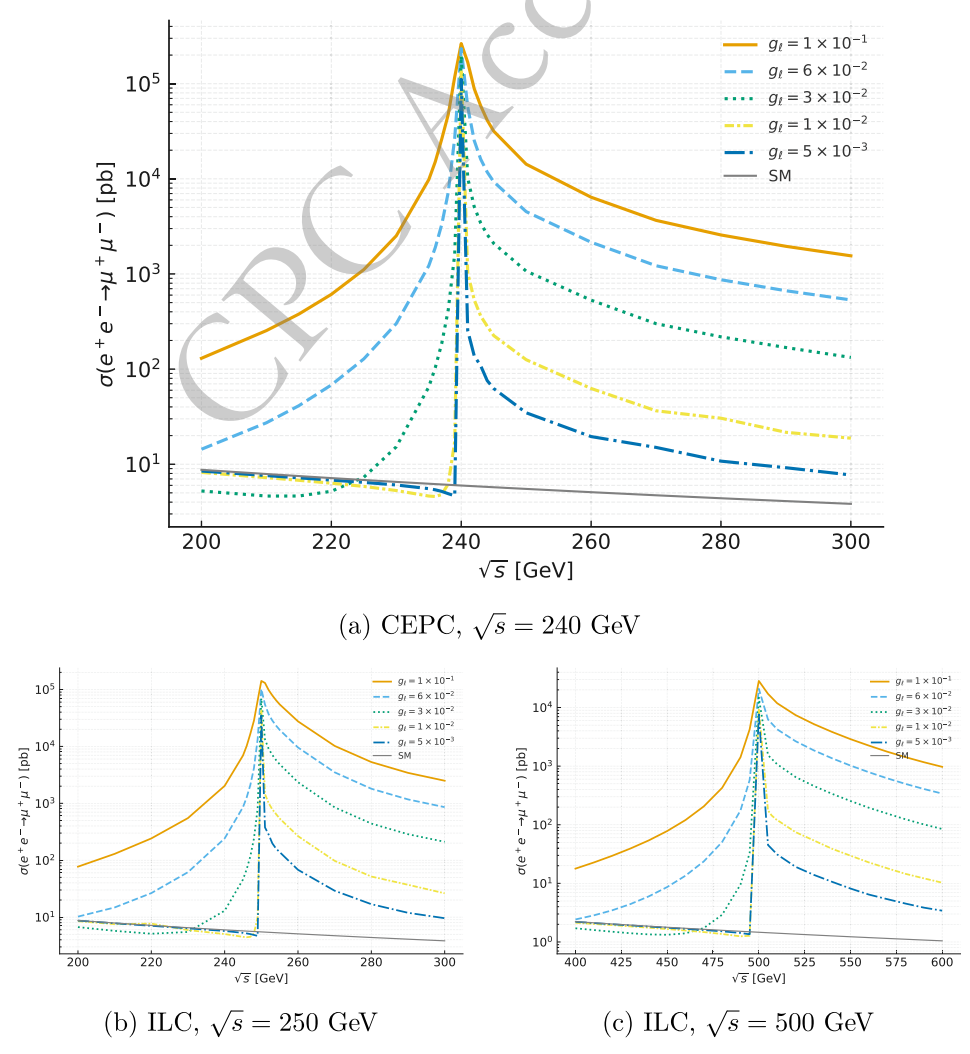


Fig. 4. (color online) Energy scans of the total cross section $\sigma(e^+e^- \to \mu^+\mu^-)$ for representative couplings g_ℓ at future e^+e^- colliders. (a) CEPC at $\sqrt{s} = 240 \text{ GeV}$ (20 ab⁻¹, TDR baseline). (b) ILC at $\sqrt{s} = 250 \text{ GeV}$ (2 ab⁻¹, polarized). (c) ILC at $\sqrt{s} = 500 \text{ GeV}$. Line styles distinguish the benchmark scenarios; the SM expectation is shown in gray.

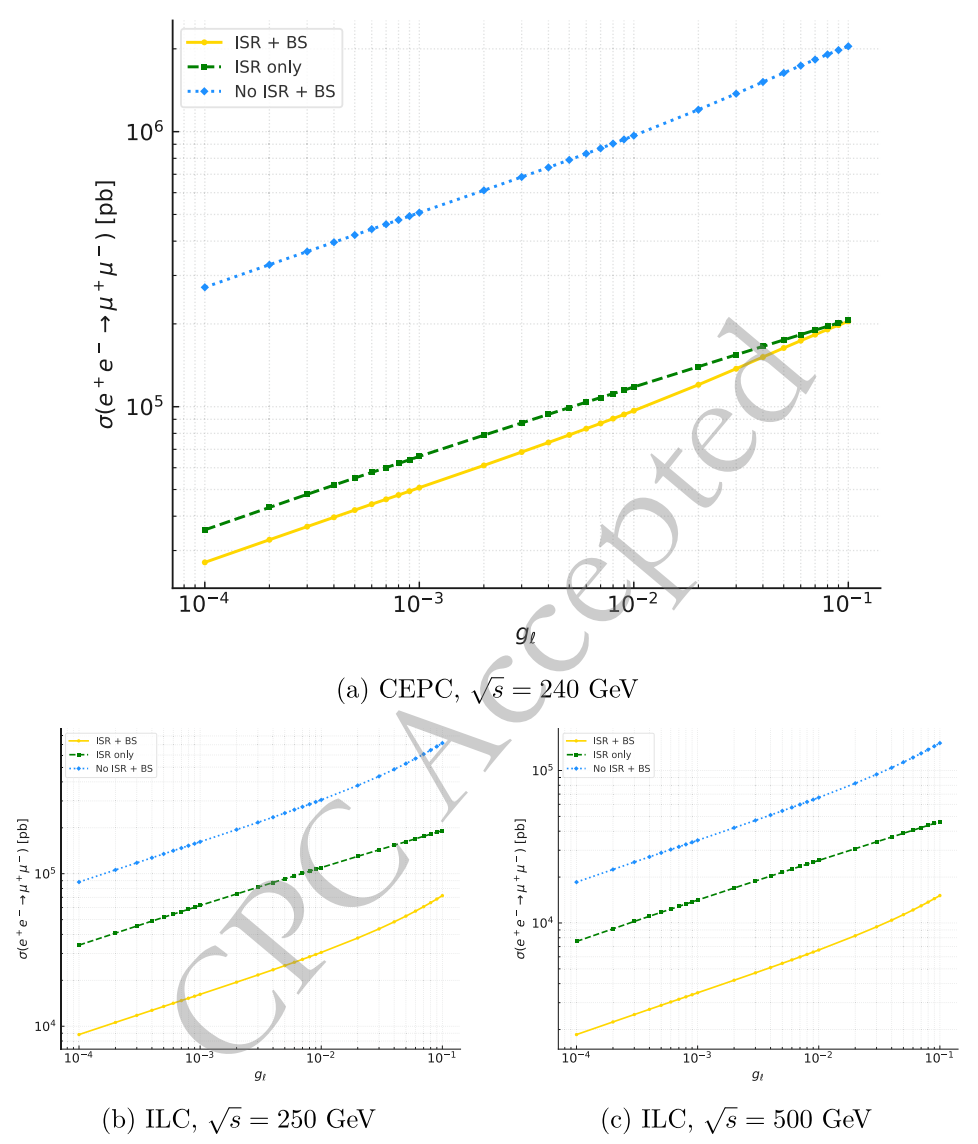


Fig. 5. (color online) Total cross section $\sigma(e^+e^- \to \mu^+\mu^-)$ as a function of the leptophilic coupling g_ℓ for CEPC and ILC setups, illustrating the impact of initial-state radiation (ISR) and beamstrahlung (BS). (a) CEPC at $\sqrt{s} = 240$ GeV, (b) ILC at $\sqrt{s} = 250$ GeV, and (c) ILC at $\sqrt{s} = 500$ GeV. Solid, dotted, and dash-dot lines correspond to the full ISR+BS simulation, ISR only, and the idealized No ISR+BS case, respectively. Both axes are displayed on logarithmic scales.

tions (Figs. 5b and 5c) exhibit a stronger sensitivity to ISR+BS, particularly at larger g_{ℓ} values. These comparisons clearly demonstrate the necessity of including realistic beam effects when estimating discovery sensitivities at future e^+e^- colliders.

The impact of ISR and beamstrahlung is illustrated in Fig. 6, where the cross section is plotted as a function of $M_{Z_{\ell}}$ for $g_{\ell} = 3 \times 10^{-2}$. At CEPC (Fig. 6a) the resonance appears as a narrow peak, while at ILC-250 (Fig. 6b) it is moderately broadened, and at ILC-500 (Fig. 6c) the peak becomes significantly wider due to stronger beam effects. In all cases, however, the deviation from the SM background remains visible, showing that ISR and beamstrahlung reduce but do not eliminate the discovery po-

tential [36, 37].

The invariant mass distribution of the di-muon pair provides a striking signature of a leptophilic resonance. Figure 7 shows the expected spectra for several representative Z_{ℓ} masses. At the CEPC (\sqrt{s} = 240 GeV, Fig. 7a), narrow peaks emerge around 180–220 GeV for g_{ℓ} = 0.02, clearly separated from the smooth Standard-Model background. The ILC-250 configuration (\sqrt{s} = 250 GeV, Fig. 7b) exhibits similar features near 200 GeV, while the ILC-500 setup (\sqrt{s} = 500 GeV, Fig. 7c) with g_{ℓ} = 0.03 demonstrates sensitivity to heavier resonances up to about 450 GeV. These distributions highlight the excellent mass resolution and discovery reach achievable at future e^+e^- colliders, with visible Z_{ℓ} peaks even for moderate coup-

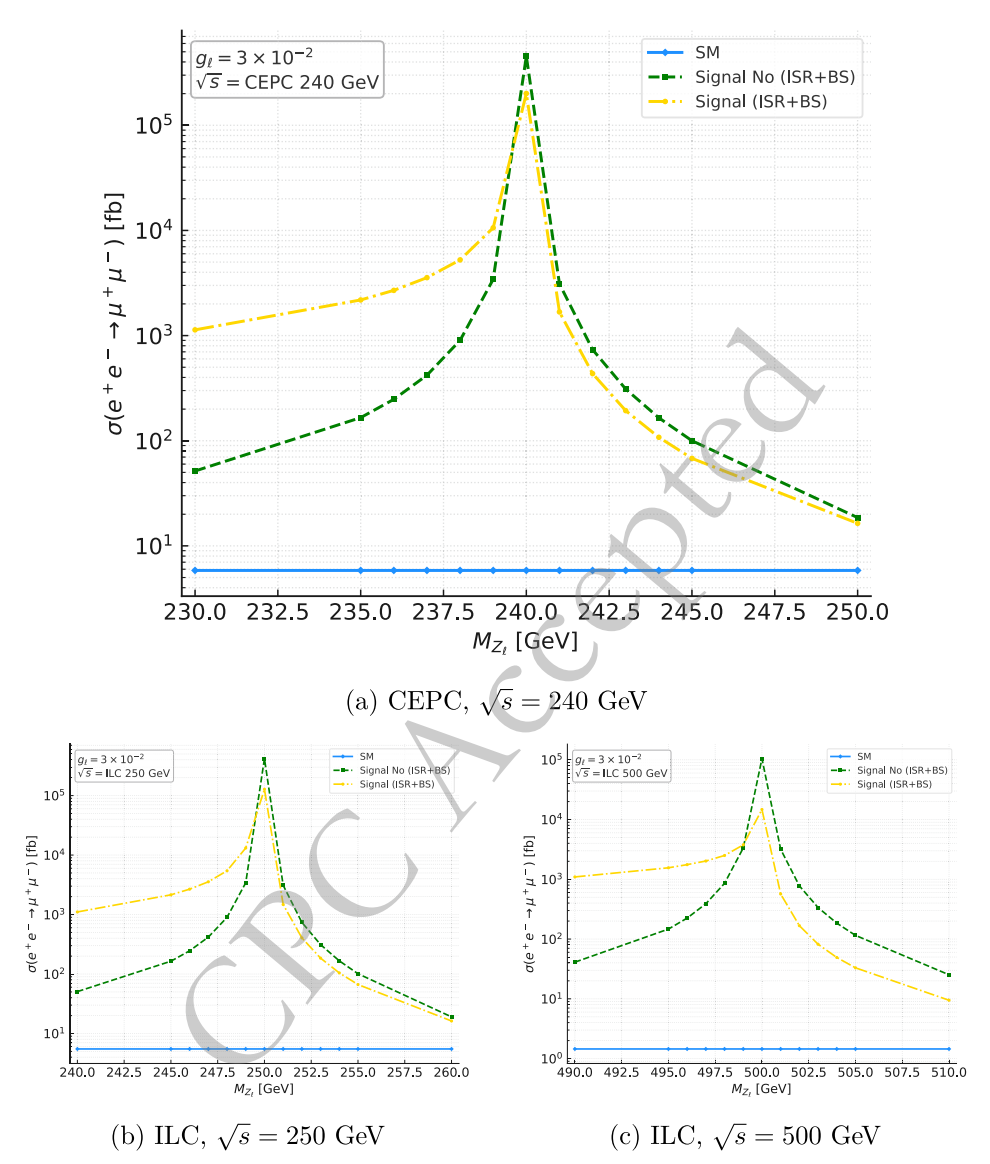


Fig. 6. Cross section $\sigma(e^+e^- \to \mu^+\mu^-)$ as a function of M_{Z_ℓ} for $g_\ell = 3 \times 10^{-2}$. Comparison shown for SM background, signal without ISR/BS, and full ISR+BS. CEPC peak remains narrow, ILC-250 broadens, and ILC-500 widens further though deviation from SM is still distinct.

lings.

V. RESULTS AND DISCUSSION

Before presenting the numerical projections, it is important to verify that the benchmark scenarios considered here are consistent with existing experimental limits. Current collider searches place only mild constraints on purely leptophilic gauge bosons, since hadron colliders are mostly sensitive to quark–coupled interactions. Dedicated dilepton resonance searches at the LHC [38, 39] typically assume universal couplings to both quarks and leptons, which are absent in our model. Consequently, direct LHC limits can be substantially relaxed, allowing sub–TeV Z_{ℓ} masses for couplings below $g_{\ell} \lesssim 0.1$. Addi-

tional constraints from LEP-II contact—interaction analyses [40] and low—energy precision data [41, 42] are also satisfied across the parameter space explored in this study. Therefore, all benchmark points used in the following analysis remain consistent with current bounds and provide a valid basis for discovery projections.

Having established the signal and background framework, we now turn to the projected sensitivities and discovery reaches for the leptophilic photon Z_{ℓ} at CEPC and ILC.

The discovery potential of future e^+e^- colliders is summarized in Fig. 8, which displays the 3σ and 5σ significance contours in the (M_{Z_ℓ}, g_ℓ) plane [25, 43–45]. At CEPC (Fig. 8a), couplings down to $g_\ell \approx 10^{-3}$ are accessible for M_{Z_ℓ} up to about 220 GeV. The ILC-250 projec-

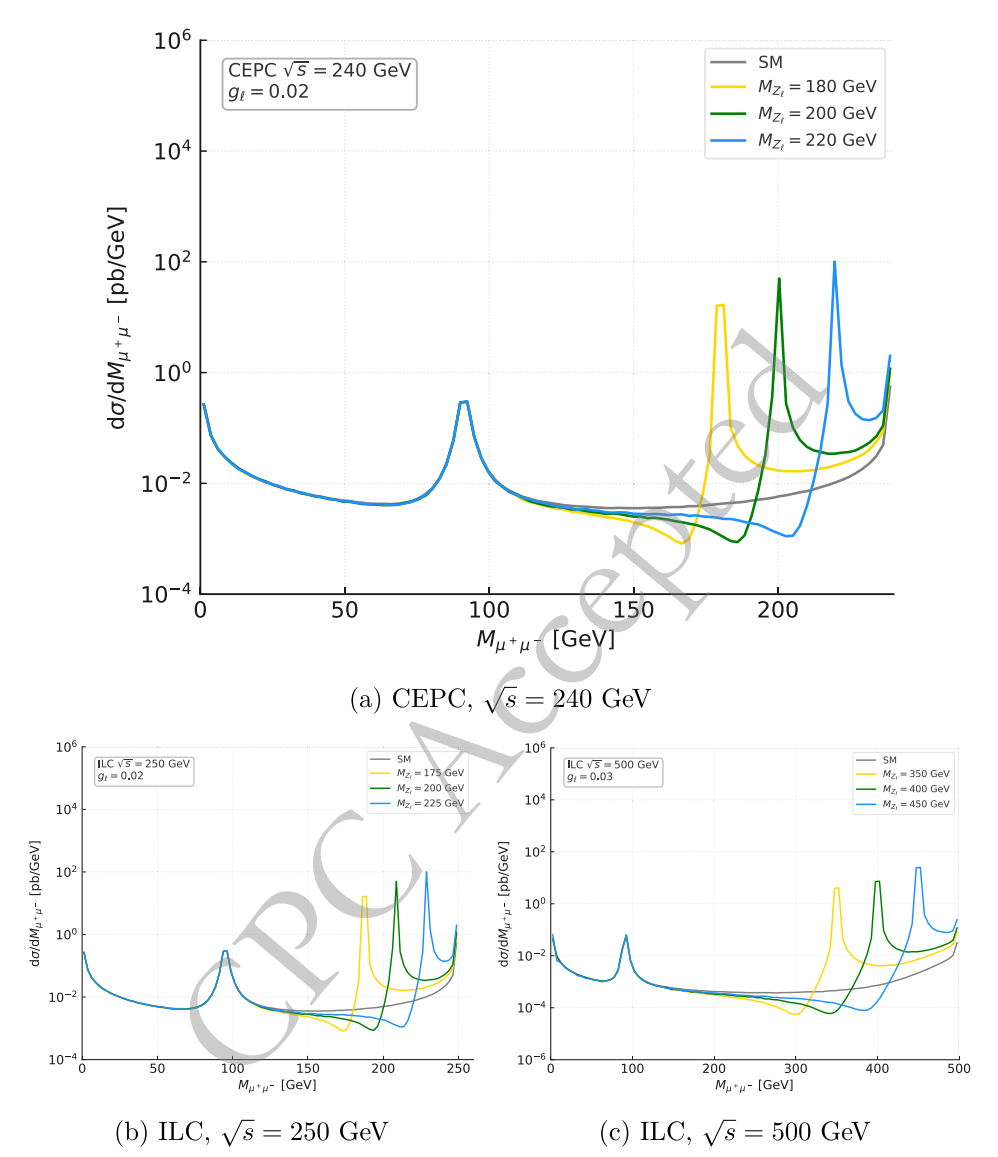


Fig. 7. Invariant mass distributions of the di-muon system for representative Z_{ℓ} benchmark masses at future e^+e^- colliders. (a) CEPC at $\sqrt{s} = 240$ GeV with $g_{\ell} = 0.02$ shows pronounced peaks in the 180–220 GeV range. (b) ILC at $\sqrt{s} = 250$ GeV displays similar structures near 200 GeV, and (c) ILC at $\sqrt{s} = 500$ GeV with $g_{\ell} = 0.03$ extends the sensitivity to resonances up to about 450 GeV. The narrow Z_{ℓ} resonances stand out clearly above the smooth Standard Model background, illustrating the discovery potential and excellent mass resolution achievable at future lepton colliders.

tion (Fig. 8b) extends the reach in mass while maintaining similar sensitivity to small couplings, and the ILC-500 setup (Fig. 8c) pushes the accessible region further into the TeV scale. These results emphasize the complementarity of circular and linear colliders in exploring the leptophilic gauge boson scenario.

In addition to the total cross section, we have also examined differential observables that are sensitive to angular effects, such as the forward–backward asymmetry $A_{\rm FB} = (\sigma_F - \sigma_B)/(\sigma_F + \sigma_B)$, where σ_F and σ_B denote the forward and backward cross sections, respectively. The interference between the SM and leptophilic amplitudes induces characteristic deviations in $A_{\rm FB}$, particularly near

the Z_{ℓ} resonance. Preliminary simulations indicate that these effects are consistent with the total-rate behavior discussed above, and can further improve the discrimination power, especially when beam polarization is available at ILC. A more detailed differential study is left for future work.

For comparison, previous sensitivity estimates at LEP and early ILC studies typically relied on parton-level simulations without full ISR and beamstrahlung effects [7, 8, 33]. The present analysis therefore represents a more realistic projection, showing that the clean di-muon channel retains robust sensitivity even once collider-specific effects are included. This improvement is particularly rel-

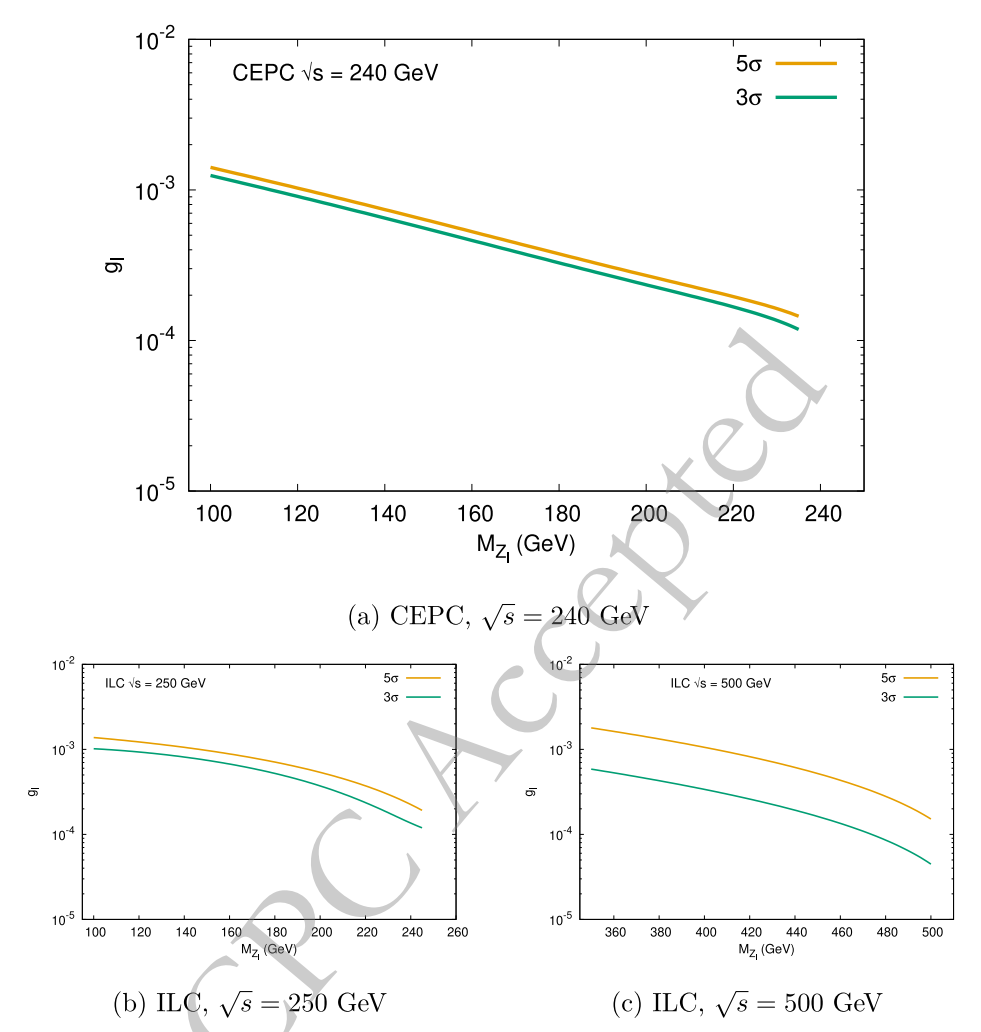


Fig. 8. Projected 3σ and 5σ discovery reaches in the (M_{Z_ℓ}, g_ℓ) plane. (a) CEPC at $\sqrt{s} = 240$ GeV demonstrates sensitivity down to $g_\ell \simeq 10^{-3}$ for $M_{Z_\ell} \lesssim 220$ GeV. (b) ILC-250 extends the mass range while maintaining comparable coupling reach, and (c) ILC-500 further improves the mass coverage up to the multi-hundred-GeV region. The curves correspond to statistical significances computed with full ISR+BS simulation, highlighting the complementarity of circular and linear e^+e^- colliders.

evant for CEPC, whose very high luminosity enhances the reach well beyond earlier expectations.

Taken together, the results presented in Figs. 2-8 provide a comprehensive picture of the discovery potential for a leptophilic photon Z_{ℓ} at future e^+e^- colliders. The energy dependence of the cross section highlights the complementary strengths of CEPC and ILC, with the former providing very high statistics at $\sqrt{s} \approx 240$ GeV and the latter extending the reach towards higher masses through its 250 and 500 GeV options. The variation of the cross section with $M_{Z_{\ell}}$ and g_{ℓ} illustrates how even moderate couplings already produce visible deviations from the SM, even after ISR and beamstrahlung are taken into account. Invariant-mass spectra confirm that narrow resonances would appear as clear peaks over the SM background, consistent with existing bounds from previous e^+e^- experiments [33, 36, 37]. Finally, the projected 3σ and 5σ contours show that CEPC can probe couplings

down to $g_{\ell} \approx 10^{-3}$ in the sub-TeV region, while the ILC pushes the accessible range further into the TeV domain. These findings underline the strong complementarity of circular and linear colliders, and establish a solid phenomenological basis for incorporating leptophilic gauge bosons into future precision programs [11, 12, 25, 26].

VI. CONCLUSIONS

We have presented a dedicated study of the discovery potential for a leptophilic gauge boson Z_{ℓ} in the clean channel $e^+e^- \rightarrow \mu^+\mu^-$ at future e^+e^- colliders. Incorporating the effects of initial-state radiation (ISR), beamstrahlung (BS), and basic detector acceptance, we have provided realistic sensitivity estimates for CEPC and ILC. The results show that CEPC, with its very high luminosity at $\sqrt{s} = 240$ GeV, offers broad coverage in the low-mass region, probing couplings down to $g_{\ell} \approx 10^{-3}$,

while the ILC extends the accessible Z_{ℓ} mass range up to the TeV scale through its 250 and 500 GeV stages. This complementarity underscores the unique role of next-generation lepton colliders in testing leptophilic gauge interactions with high precision.

Our analysis establishes a clear benchmark for the cleanest leptonic final state and demonstrates that even after including realistic beam effects the Z_{ℓ} signal remains clearly visible above the SM background. These findings provide a solid phenomenological basis for future strategies in exploring purely leptophilic scenarios at high-energy colliders.

Compared with previous parton-level estimates and earlier sensitivity projections from LEP and ILC studies, the present work offers a more realistic evaluation by incorporating ISR, BS, and acceptance effects. In this respect, our results represent the first direct side-by-side comparison of CEPC and ILC in the context of a purely leptophilic gauge boson. The projections presented here highlight the advantage of CEPC in probing very small

couplings at low mass, and the complementary role of ILC in extending the discovery reach well into the multihundred GeV domain.

From a broader perspective, the analysis provides timely input to the global discussion on the physics potential of future lepton colliders. In particular, CEPC, as a central project in China, is shown to deliver world-leading sensitivity to new leptonic forces in the sub-TeV regime, while the ILC offers a complementary path at higher energies. Taken together, these findings underline the importance of pursuing both circular and linear collider options and establish a strong phenomenological basis for including leptophilic gauge bosons in the physics case of next-generation facilities.

DATA AVAILABILITY

All data generated and analyzed in this study are included in the article. Additional simulation inputs and numerical results are available from the corresponding author upon reasonable request.

References

- Navas S, et al., Phys. Rev. D 110, 030001 (2024)
- [2] Fukuda Y, et al., Phys. Rev. Lett. 81, 1562 (1998)
- Ahmad Q R, et al., Phys. Rev. Lett. 89, 011301 (2002) [3]
- [4] Lee T D and Yang C N, Phys. Rev. 98, 1501 (1955)
- [5] Okun L B, Sov. Phys. JETP 29, 1 (1969).
- [6] Fayet P, Phys. Lett. B 95, 285 (1980) Langacker P, Rev. Mod. Phys. 81, 1199 (2009) [7]
- [8] Heeck J and Rodejohann W, Phys. Rev. D 84, 075007 (2011)
- Altmannshofer W, et al., JHEP 12, 044 (2014)
- [10] Bauer M and Neubert M, Phys. Rev. Lett. 120, 141802 (2018)
- [11] CEPC Collaboration 2018 (Preprint arXiv: 1809.00285)
- Behnke T et al. 2013 (Preprint arXiv: 1306.6327) [12]
- [13] Okun L B, Sov. Phys. Usp. 12, 427 (1970)
- [14] Holdom B, Phys. Lett. B 166, 196 (1986)
- Foot R and He X G, Phys. Lett. B 267, 509 (1991) [15]
- Allanach B C, Davighi J and Melville S, JHEP 02, 082 [16] (2019)
- Adler S L, Phys. Rev. 177, 2426 (1969) [17]
- Bell J S and Jackiw R, Nuovo Cim. A 60, 47 (1969) [18]
- Bouchiat C, Iliopoulos J and Meyer P, Phys. Lett. B 38, 519 [19] (1972)
- Preskill J, Ann. Phys. 210, 323 (1991) [20]
- [21] Qiu D and Tang Y, JHEP **2024**, 167 (2024)
- [22] Cai C, He H J, Ren J and Zhu W, Phys. Rev. D 106, 095003 (2022)
- [23] Hook A, Phys. Rev. D 84, 055003 (2011)
- [24] Kara S O 2025 (*Preprint* arXiv: 2508.18496)

- [25] Abada A, et al., Eur. Phys. J. ST 228, 261 (2019)
- Aicheler M et al. 2012 Tech. Rep. CERN-2012-007 CERN [26]
- [27] Skrzypek M and Jadach S, Z. Phys. C 49, 577 (1991)
- [28] Kuraev E A and Fadin V S, Sov. J. Nucl. Phys. 41, 466
- [29] Yokoya K and Chen P 1992 Tech. Rep. SLAC-PUB-4935 SLAC
- Belyaev A, Christensen N D and Pukhov A, Comput. Phys. [30] Commun. 184, 1729 (2013)
- [31] Alwall J, et al., JHEP 07, 079 (2014)
- Kilian W, Ohl T and Reuter J, Eur. Phys. J. C 71, 1742 [32]
- ALEPH, DELPHI, L3, Collaborations O and Group L E W [33] 2003 (*Preprint* arXiv: hep-ex/0312023)
- [34] Cowan G, Cranmer K, Gross E and Vitells O, Eur. Phys. J. C 71, 1554 (2011)
- Read A L, J. Phys. G 28, 2693 (2002) [35]
- Lees J P, et al., Phys. Rev. Lett. 113, 201801 (2014) [36]
- [37] Kou E, et al., Prog. Theor. Exp. Phys. 2019, 123C (2019)
- [38] Aad G, et al., JHEP 10, 182 (2019), arXiv: 1903.06248
- [39] Sirunyan A M, et al., JHEP 07, 208 (2021), arXiv: 2103.02708
- Schael S, et al., Phys. Lett. B 565, 61 (2003), arXiv: hep-[40] ex/0306031
- Lees J P, et al., Phys. Rev. Lett. 113, 201801 (2014), arXiv: [41] 1406.2980
- Abi B, et al., Phys. Rev. Lett. 126, 141801 (2021), arXiv: [42] 2104.03281
- [43] Group C S 2018 (*Preprint* arXiv: 1811.10545)
- Barklow T et al. 2015 (Preprint arXiv: 1506.07830) [44]
- de Blas J et al. 2018 (Preprint arXiv: 1812.02093) [45]